JOURNAL OF THERMOPHYSICS AND HEAT TRANSFER
Vol. 7, No. 1, Jan.–March 1993

Total Thermal Radiation Absorption by a Single Spherical Droplet

P. L. C. Lage* and R. H. Rangel†
University of California, Irvine, Irvine, California 92717

The total energy absorption distribution inside a liquid droplet irradiated by blackbody emission is determined by spectral and solid angle integrations of the spectral absorption distribution given by electromagnetic theory. Total absorptances are calculated from volume integration of the absorption distribution and from efficiency factor spectral integration. Results are presented for 1–100 μm radius n-decane and water droplets irradiated by a blackbody at 850–2000 K, in several axisymmetric configurations. Under spherically symmetric irradiation conditions the water absorption results are used to verify the applicability and accuracy of the geometrical-optics approximation through comparison with those results. The band characteristics of decane absorption are also analyzed. It is verified that the trapezoidal quadrature is usually a good approximation for spectral integration. The geometrical-optical approach leads to total absorptance values with errors larger than 10% for droplets smaller than 25 μm. Only the two principal bands of decane, including their wings, are needed to fairly well predict total absorption distribution in decane droplets.

Nomenclature

c_n, d_n = internal electric field vector series coefficients
$\boldsymbol{E}$ = internal electric field vector
E_r, E_θ, E_ϕ = internal electric field vector spherical components
E_0 = incident electric field amplitude
$\mathcal{F}_\lambda$ = blackbody fraction between 0 and λ
G = geometric cross section, πR^2
$\mathcal{G}$ = total incident irradiance
I = intensity of radiation
i = $\sqrt{-1}$
k = imaginary part of complex refractive index
m = relative complex refractive index, N/N_0
N = complex refractive index, $n + ik$
P_n = Legendre polynomial
Q = absorption distribution
$\langle Q \rangle$ = mean volumetric absorption
$\mathcal{Q}$ = efficiency factor
R = droplet radius
$\mathcal{R}$ = real part operator
r = radial coordinate
S = dimensionless radiation absorption distribution, $Q/\langle Q \rangle$
T = temperature
V = droplet volume
W = energy
x = size parameter, $2\pi R/\lambda$
z = coordinate along wave propagation direction
α = absorptance
ε = emissivity
η = dimensionless radial coordinate, r/R
Θ = polar angle within which the droplet views the source
θ = polar coordinate
ϑ = magnetic permeability
λ = wavelength
μ = cos θ
ξ_n = Bessel-Ricatti function of the third kind, $\psi_n + i\chi_n$
Π = angular function
ρ = dimensionless radial coordinate, $2\pi Nr/\lambda$
σ = Stefan-Boltzmann constant
τ = angular function
ϕ = azimuthal coordinate
χ_n = Bessel-Ricatti function of the second kind
ψ_n = Bessel-Ricatti function of the first kind
Ω = solid angle

Subscripts

a = absorbed
b = blackbody
back = back absorption peak
front = front absorption peak
V = volume-integrated
λ = spectral
0 = relative to the surrounding medium, incident

Superscript

$'$ = directional radiation or derivative

Introduction

IN typical liquid-fueled combustors and heat and mass transfer processes (including interactions among gas and liquid phases) combustor walls and particles (soot) occur at elevated temperatures at which radiative effects are significant. The problem of spray vaporization and combustion, particularly the single-droplet problem, has been intensively analyzed in the past few years under both convective and stagnant environments.[1–4] Some models have been developed for the heat and mass transfer phenomena in both the liquid and gas phases[5,6] which are suitable for global combustor simulation. However, the liquid-phase analyses have neglected the thermal radiation absorption inside the droplet.

The absorption of electromagnetic energy by spheres irradiated by monochromatic plane waves has been theoretically and experimentally investigated by many authors in the past few years. Dusel et al.[7] have calculated the absorption distribution for small absorbing spheres (x = 0.1–5.0). The existence of absorption centers due to highly nonuniform absorption has been verified. Pendleton[8] has used the nonuni-

Received Dec. 20, 1991; revision received March 27, 1992; accepted for publication March 31, 1992.

*Junior Specialist, also Assistant Professor on leave from Department of Chemical Engineering, COPPE/UFRJ, 21945 Rio de Janeiro, P.O. Box 68502, Brazil.

†Assistant Professor, Department of Mechanical and Aerospace Engineering. Senior Member AIAA.

form absorption distribution to explain the explosive vaporization of water droplets irradiated by a pulsed CO_2 laser experimentally observed by Kafalas and Ferdinand.[9] More recently, the absorption distribution regimes have been characterized by Tuntomo et al.[10] for a wide range of absorption index k, and size parameter x. They have distinguished three types of absorption regimes: 1) uniform, 2) back-concentrated, and 3) front-concentrated absorption. These definitions employ a reference frame placed in the droplet, therefore, front refers to the illuminated side and back to the dark side of the droplet. A regime map is given that predicts the absorption regime based on the values of the size parameter and the absorption index. Tuntomo et al.[10] have verified that the geometrical-optics approximation can lead to considerable error in the spectral radiation absorption distribution. They have empirically verified that it is necessary that $x \geq 20n^3$ ($1 < n \leq 2$ and $0.001 \leq k \leq 1$), for a 20% error in the spectral absorption distribution and total absorptance calculated using geometric optics.

The radiative absorption distribution inside a droplet irradiated by a blackbody under conditions of spherical symmetry has been determined[11] for water droplets using the geometrical-optics approximation. For spherical symmetry, the absorption distribution in a homogeneous sphere can also be calculated as a special case by the procedure given by Mackowski et al.[12] for stratified spheres. Sitarski[13] has obtained the absorption distribution inside a coal-water slurry droplet irradiated by a blackbody from a single direction, using electromagnetic wave theory. The spectral integration used was a simple Riemann sum using 12 spectral locations. Recently, Sitarski[14] has analyzed the vaporization of a coal-water slurry droplet irradiated by blackbody radiation within a 2π solid angle (which physically corresponds to irradiation from a black plane). The total hemispherical absorption distribution was approximated by the directional absorption distribution for a total intensity equivalent to the intensity of the irradiation upon the droplet from the solid angle 2π.

In the present work, the total radiation absorption distributions for water and decane droplets are calculated for several blackbody temperatures, droplet sizes, and axisymmetric configurations. Total absorptances for directional blackbody irradiation are also calculated from the total absorption distribution and from efficiency factor spectral integration. The main goal is to obtain bench mark absorption distribution results to be used in droplet vaporization analyses.[15] The electromagnetic wave theory can then be used to rigorously calculate the total directional radiation absorption distribution if the following assumptions are made:

1) Directionally incident radiation is approximated as a superposition of monochromatic unpolarized plane waves with a blackbody spectral intensity distribution. 2) The medium between the droplet and the flame front is nonparticipating. 3) The droplet is considered a linear, isotropic, and homogeneous sphere (the electrical conductivity, magnetic permeability, and electric susceptibility of the sphere do not depend on the electric vector field, direction, and spatial position).

Moreover, due to low droplet temperatures, radiation emission by the droplet is neglected. The blackbody spectral distribution of intensity has been chosen to avoid the time-consuming radiation emission calculation for a specific flame. It gives the maximum emission for a given reference temperature and can be used as a upper limit for incident thermal radiation. It should be noted that the blackbody spectral distribution and nonparticipating medium assumptions are not fulfilled in combustion environments. At most, a gray-like emission behavior may be attributed to a luminous flame, and gas and soot almost always render the medium participating. However, no exact solution for the Maxwell equations is available for an absorbing sphere in a participating medium, and assumption 2) is necessary to use the Mie theory. However, it is believed that the results will represent the trends of absorption behavior of a droplet in a combustion environment.

A solid angle integration suffices for the total hemispherical absorption distribution in axisymmetric configurations. Care is taken in both spectal and solid angle integrations in order to achieve bench mark absorption results. The present work evaluates the accuracy of geometrical optics approach in determining total absorption values, through comparison with Harpole's results[11] and provides the necessary input for droplet vaporization studies. In addition, the applicability and accuracy of some desirable approximations (the simple trapezoidal rule for spectral integration and the absorption-band analysis for decane), are determined.

Internal Radiation Absorption Distribution

For each wavelength, the spherical components of the internal electric field vector are given by (Dusel et al.[7] and Bohren and Huffman[16]

$$E_r = -\frac{E_0 \cos\phi}{\rho^2} \sum_{n=1}^{\infty} d_n i^{n+1}(2n+1) P_n^1(\cos\theta)\psi_n(\rho) \tag{1}$$

$$E_\theta = -\frac{E_0 \cos\phi}{\rho} \sum_{n=1}^{\infty} \frac{i^{n+1}(2n+1)}{n(n+1)} [d_n \tau_n(\theta)\psi_n'(\rho) + i c_n \Pi_n(\theta)\psi(\rho)] \tag{2}$$

$$E_\phi = \frac{E_0 \sin\phi}{\rho} \sum_{n=1}^{\infty} \frac{i^{n+1}(2n+1)}{n(n+1)} [d_n \Pi_n(\theta)\psi_n'(\rho) + i c_n \tau_n(\theta)\psi_n(\rho)] \tag{3}$$

where the prime denotes differentiation with respect to the argument, and $\theta = 0$ is the direction of propagation. The angular functions are expressible in terms of Legendre polynominals

$$\Pi_n(\theta) = \frac{P_n^1(\cos\theta)}{\sin\theta} \qquad \tau_n(\theta) = \frac{dP_n^1(\cos\theta)}{d\theta} \tag{4}$$

and the series coefficients are

$$c_n = \frac{\vartheta m[\psi_n(x)\xi_n'(x) - \xi_n(x)\psi_n'(x)]}{\vartheta\psi_n(mx)\xi_n'(x) - \vartheta_0 m\xi_n(x)\psi_n'(mx)} \tag{5}$$

$$d_n = \frac{\vartheta m[\psi_n(x)\xi_n'(x) - \xi_n(x)\psi_n'(x)]}{\vartheta_0 m\psi_n(mx)\xi_n'(x) - \vartheta\xi_n(x)\psi_n'(mx)} \tag{6}$$

Using the cross-product property of the Bessel functions, the series coefficients can be further simplified to the following expressions:

$$c_n = \frac{mi}{\psi_n(mx)\xi_n'(x) - (\vartheta_0/\vartheta)m\xi_n(x)\psi_n'(mx)} \tag{7}$$

$$d_n = \frac{mi}{(\vartheta_0/\vartheta)m\psi_n(mx)\xi_n'(x) - \xi_n(x)\psi_n'(mx)} \tag{8}$$

Once the internal electromagnetic field is known, one can determine the energy absorption distribution inside the sphere for the given wavelength of incident radiation. It can be shown that (Dusel et al.[7])

$$Q_\lambda' = \frac{4\pi k I_{0\lambda}}{\lambda} \Re\left\{m\frac{\vartheta_0}{\vartheta}\right\} \left|\frac{E}{E_0}\right|^2 \tag{9}$$

where $|E/E_0|^2$ is the dimensionless source function and $\Re\{m(\vartheta_0/\vartheta)\}$ simplifies to n when $\vartheta = \vartheta_0$.

Here, we assume $\vartheta = \vartheta_0$, and for unpolarized incident radiation, which is the case of thermal radiation, it can be shown[17] that ϕ should be set to $\pi/4$.

The total energy absorption distribution for directionally incident radiation is given by

$$Q'(\eta, \theta) = \int_0^\infty Q'_\lambda(\eta, \theta)\, d\lambda \tag{10}$$

This integral can be transformed into a integral in terms of blackbody fraction

$$Q'(\eta, \theta) = 4\sigma T^4 \int_0^1 \frac{k\varepsilon_\lambda n_0^2}{\lambda} \Re\left\{m\frac{\vartheta_0}{\vartheta}\right\} \left|\frac{\boldsymbol{E}}{\boldsymbol{E}_0}\right|^2 d\mathcal{F}_\lambda \tag{11}$$

where $\mathcal{F}_\lambda$ is the fraction of blackbody radiation between 0 and λ, and thus $\lambda = \lambda(\mathcal{F}_\lambda)$. For blackbody irradiation $\varepsilon_\lambda = 1$.

Then the total hemispherical absorption distribution is obtained by integrating Q' over the solid angle for which there is irradiation upon the droplet. Thus, we have

$$Q(\eta, \mu, \phi) = \int_{\Delta\Omega_0} Q'(\eta, \bar{\mu})\, d\Omega_0 \tag{12}$$

where

$$\bar{\mu} = \mu\mu_0 + (1 - \mu^2)^{1/2}(1 - \mu_0^2)^{1/2} \cos(\phi - \phi_0) \tag{13}$$

Since the irradiation is considered axisymmetric, Q does not depend on ϕ. Moreover, in the case of spherically symmetric irradiation, it does not depend on μ either. Accordingly

$$Q(\eta) = 2\pi \int_{-1}^1 Q'(\eta, \mu_0)\, d\mu_0 \tag{14}$$

The total hemispherical absorptance is defined by

$$\alpha = \frac{W_a}{\mathcal{G}G} = \frac{4}{3}\frac{R\langle Q\rangle}{\mathcal{G}} \tag{15}$$

The mean volumetric radiation absorption $\langle Q\rangle$, is obtained by integration over the droplet volume of the total hemispherical absorption distribution

$$\langle Q\rangle = \frac{1}{V}\int_V Q(r, \mu)\, dV \tag{16}$$

Since we are considering the same blackbody irradiation for every direction, α is identical to the directional total absorptance α', defined as

$$\alpha' = \frac{W'_a}{I_0 G} = \frac{4}{3}\frac{R\langle Q'\rangle}{I_0} \tag{17}$$

The directional total absorption can be calculated, alternatively, from the spectral integration of the absorption efficiency factor

$$\alpha' = \frac{\int_0^\infty \mathcal{Q}'_{a\lambda} I_{0\lambda}\, d\lambda}{\int_0^\infty I_{0\lambda}\, d\lambda} \tag{18}$$

which again can be simplified for blackbody incident radiation, using the blackbody fraction $\mathcal{F}$

$$\alpha' = \int_0^1 \mathcal{Q}'_{a\lambda}[\lambda(\mathcal{F})]\, d\mathcal{F} \tag{19}$$

The $\mathcal{Q}'_{a\lambda}$ value is obtained by the difference from the extinction and scattering efficiency factors.[16]

It is interesting to define a dimensionless absorption distribution by

$$S = \frac{Q}{\langle Q\rangle} \tag{20}$$

As a result, we have

$$\frac{1}{V}\int_V S\, dV = 1 \tag{21}$$

Note that $S = 1$ implies uniform radiation absorption inside the droplet. The dimensionless absorption distribution definition allows the separation of the radiation absorption effect into two parts: 1) the total energy absorbed by the droplet, given by $\langle Q\rangle$ (or α), and 2) the nonuniform dimensionless absorption S. This separation has proved to be useful in the droplet vaporization analysis.[15]

Numerical Procedure

A difficulty in the calculation of spectral distribution of radiation absorption by Eq. (9) is due to the numerical instability of the forward recursive scheme for calculating the Bessel-Ricatti function of the first kind $\psi_n(z)$ and its logarithmic derivative function $D_n(z)$,[16] which is utilized in the computation of $\psi'_n(z)$. Here we used the criterion devised by Wiscombe[18] based on the size parameter and relative refractive index that allows the choice, a priori, between forward recursion (stopped before the occurrence of numerical instability) and downward recursion (initialized by the Lentz method[19]). The forward recursion in $\xi_n(x)$, for real argument, and in the angular functions $\tau_n(\theta)$ and $\pi_n(\theta)$ has no numerical instability problems,[16,19] and thus it is adopted.

The integration of the spectral energy absorption distribution of Eq. (11) could be performed only for the given range of refractive index data. The basic set of interlacing optimal abscissa collocation quadratures given by Patterson[20] has been used to build an automatic integrator using a global error convergence criterion and interval subdivision by three. This integrator can handle the integration of a vector function of one variable which enables it to integrate the spectral absorption distribution. Since the most computationally intensive task is the evaluation of the spherical Bessel functions for complex argument, and since a typical mesh has 1000–2000 points inside the droplet, the simultaneous integration of the spectral absorption at all mesh points saves an enormous amount of computational time. This integrator has been tested using the same test integrands given by Patterson.[21] It has been verified to be as efficient as QSUBA and CADRE,[21] and it is also reliable for any required accuracy. It has also been used to spectrally integrate the absorption efficiency factor [Eq. (19)]. Trapezoid quadrature, based on the wavelengths where the optical contants are known, is also used to perform the spectral integration in order to verify its applicability.

The total hemispherical absorption distribution [Eq. (12)] for an axisymmetric configuration can be expressed as

$$Q(\eta, \mu) = 2\int_{\mu_{0_{\min}}}^1 \int_1^1 (1 - \omega^2)^{-1/2} Q'(\eta, \bar{\mu})\, d\omega\, d\mu_0 \tag{22}$$

where

$$\bar{\mu} = \mu\mu_0 + (1 - \mu^2)^{1/2}(1 - \mu_0^2)^{1/2}\omega \tag{23}$$

and $\omega = \cos\phi_0$ and $\mu_{0_{\min}} = -\cos\Theta$. The quantity of $2\pi(1 - \mu_{0_{\min}})$ is the axisymmetric solid angle within which there is blackbody irradiation incident upon the droplet. The integration over ω is performed by Gauss-Tschebyscheff quadrature,[22] and the resulting angle μ_0 integral is carried out using the automatic integrator. A sequence of ascending Tsche-

byscheff quadrature orders with the automatic integrator error control is used to assure an accuracy always better than 0.1% in the double integration. The integrand values at the quadrature abscissae are calculated by linear interpolation between neighboring points. In order to check if the chosen grid was fine enough, directional and hemispherical absorption results for 50 and 100 quadrature points have been compared and no appreciable deviation was found, the results being always within 1%. Another check for the solid-angle numerical procedure was to compare its results for spherically symmetric irradiation to those obtained by Eq. (14), using single Lobatto quadrature. Both hemispherical absorption distributions agreed within 0.1%.

The total absorption is always calculated at Lobatto quadrature points in μ and at Radau quadrature abscissae at η^2. This radial transformation concentrates the points near the surface, where the energy absorption distribution varies fast. Typically, 20 points in the radial direction and 50–100 points in μ have been used. Thus, a Radau quadrature over η^2 and a Lobatto quadrature over μ are sufficient to determine the mean volumetric radiation absorption based on the absorption distribution.

Results

In order to calculate the total absorption distribution, it is necessary to know the optical constants for all wavelengths where the incident is not negligible. The choices of water and decane as basic substances in the analysis have two main reasons: 1) they represent two different absorption behaviors (water being highly absorptive and decane absorbing quite weakly), and 2) their optical constants are available. The optical properties for water are taken from Hale and Querry[23] and the wavelength intervals are chosen in order to obtain a blackbody fraction larger than 99%. The decane optical properties are obtained from Tuntomo.[24] Since these properties are given only for the 2.6–15 μm wavelength range, the radiation absorption calculations for decane do not include all the blackbody emission (80% for T_b = 1000 K and 53% for T_b = 1500 K). However, the near-infrared region should not have appreciable band structure, because the important decane bands due to C—H and C—C bond bending and stretching are located above 2.6 μm. Thus, although there should be some radiation absorption below 2.6 μm, the error caused by the neglect of this wavelength region should not be large (especially for low T_b). In both cases, a "not-a-knot" spline interpolation[22] based on the tabulated data has been used in the calculations. For the sake of completeness we reproduce the optical-constant data in Figs. 1 and 2 for water and decane, respectively.

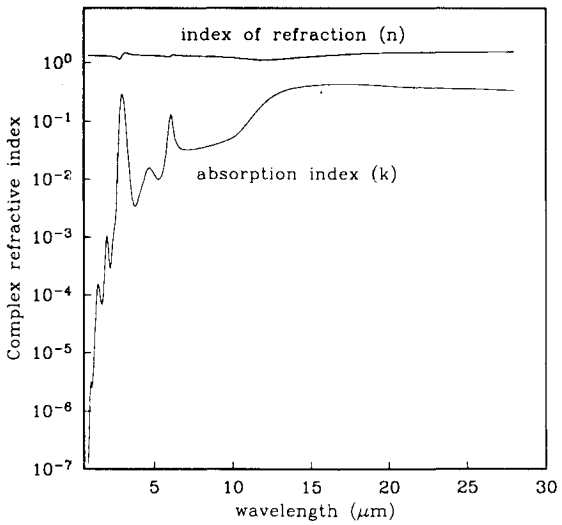

Fig. 1 Liquid water optical constants.

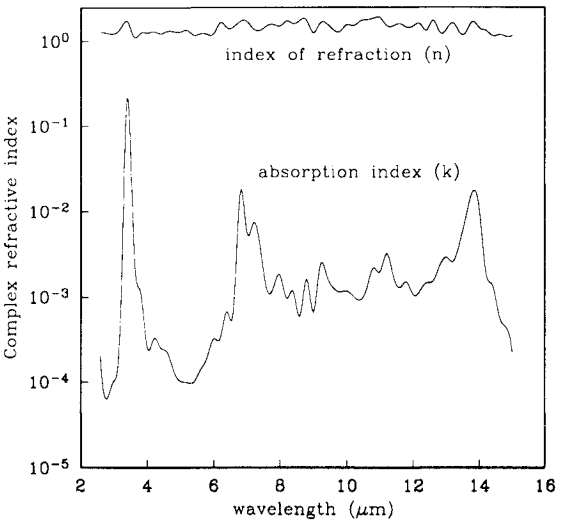

Fig. 2 Liquid decane optical constants.

The droplet size range has been chosen to match the sizes usually found in sprays. The spectrally-integrated absorption distributions for decane have been obtained for the 1–100 μm droplet radius range for blackbody irradiation at 1000 and 1500 K. For water, converged total absorption distributions could be obtained only for the 1–50 μm radius range for blackbody irradiation at 850, 1050, 1250, 1450, 1700, and 2000 K. It is believed that the truncation error in the electromagnetic field series solution, using Wiscombe's criteria,[18] together with the round-off error due to the large number of spectral absorption distribution evaluations, is the reason why the automatic integrator was not able to give a converged result for larger droplet sizes. In order to compare the total absorptances given by electromagnetic theory with those obtained by Harpole using geometrical optics,[11] total absorptances have been calculated from efficiency factors [Eq. (18)], for the 1–1500 μm radius range. Trapezoidal quadrature has also been used to integrate the spectral distributions for water droplets. However, the same deterioration of the results due to round-off errors has been obtained for sizes above 100 μm radius, as evidenced by total absorptance values greater than one.

The total energy absorption distributions are presented here in three forms: 1) three-dimensional perspective projections (not in the same scale) of the absorption in a slice through a meridional plane (cross-section projection); 2) the variation of the local absorption with angular position, for various radial positions; and 3) the variation of the local absorption with radial position. The three-dimensional projections are in different linear scales and are shown only to illustrate the absorption distribution pattern. In all figures, except those with spherically symmetric irradiation results, the incident blackbody radiation comes from left to right. The spectral energy absorption distribution results have been compared to those obtained by Tuntomo[24] and Tuntomo et al.[10] for various size parameters and complex refractive index values. The agreement between both calculations is excellent.

The total absorption distribution for a 50-μm-radius decane droplet directionally irradiated by a blackbody at 1500 K is shown in Fig. 3 (1% accuracy). It can be seen that both the front and backward absorption patterns coexist, which has been verified for decane and water droplets directionally irradiated by a blackbody at 1000–2000 K. The front absorption is dominant only for large water droplets ($\bar{R}$ = 50 μm). Figures 4 and 5 show the directional absorption distribution for decane droplets irradiated by a blackbody at 1500 K (1% accuracy) and water droplets irradiated by a blackbody at 1450 K (1% accuracy for droplets smaller than 50 μm in radius and 5% for the 50-μm-radius droplet), respectively. The smaller the droplet, the more uniform the absorption inside the drop-

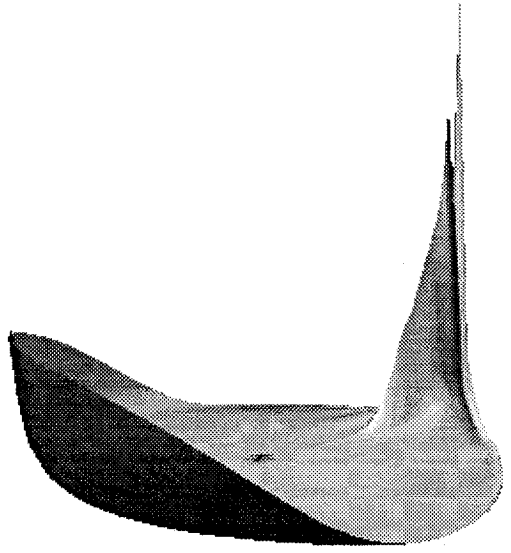

Fig. 3 Total absorption distribution for a 50-μm-radius decane droplet directionally irradiated by blackbody radiation at 1500 K.

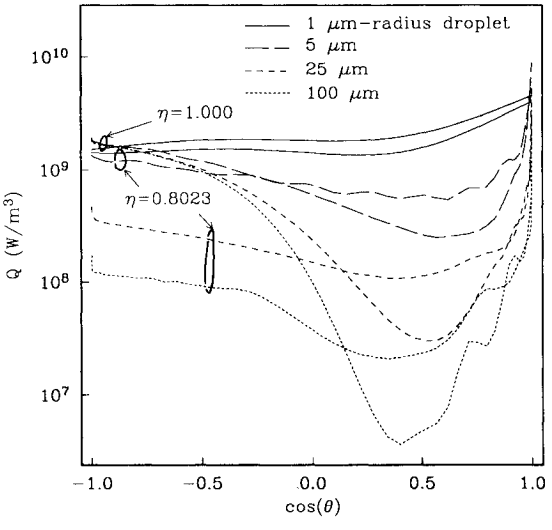

Fig. 4 Total absorption distribution for decane droplets directionally irradiated by blackbody radiation at 1500 K.

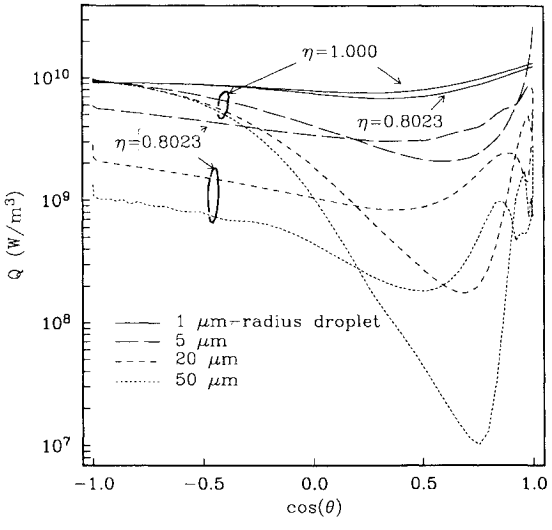

Fig. 5 Total absorption distribution for water droplets directionally irradiated by blackbody radiation at 1450 K.

let. However, above 5 μm in radius, the water and decane droplets show regions of concentrated absorption in both the droplet illuminated and dark halves.

Liquid decane infrared absorption is mainly characterized by two important bands: the C—H stretching band, located at 3.4 μm, and the C—H bending band at 6.8 μm. In order to verify the influence of band absorption in the overall absorption distribution, calculations have been performed for the decane bands which are compared with the results obtained using the 2.6–15.0 μm wavelength region. In the absorption calculation the wavelength intervals for these bands have been chosen in order to include the band wings (all the points around the band head whose k values are larger than 10^{-3}). Table 1 gives the band widths, the mean absorption, and the front and back absorption maxima for 25-μm-radius droplet directionally irradiated by a blackbody at 1000 K (1% of accuracy). It can be seen that the calculation with only the 3.4-μm band severely underestimates the absorption, especially near the back surface and inside the droplet. The addition of the second band remarkably improves the results, although it corresponds to a small blackbody fraction. However, the absorption inside the droplet is still underestimated by 40–50%, although these small absorption values are not important in the droplet thermal behavior. Table 1 shows that the absorption underestimation for the surface varies from 10 to 24% and that it is around 19% for the mean absorption value. Since the basic trends are present in the two-band results, this implies that a moderately accurate band absorption model may be developed to be used in engineering applications. It should be noted that for spectrally noncontinuous incident radiation (like the emission of a nonluminous flame) care should be taken in the use of the two-absorption-band approximation for liquid decane due to the possible mismatch between spectral regions where source emission and decane absorption take place.

Total hemispherical absorption distributions have been obtained for water and decane droplets in various configurations. Representative results are shown in Fig. 6 for a 50 μm decane droplet irradiated by a blackbody at 1500 K for several irradiation solid angles. Figure 6 shows the variation of the absorption along the main droplet axis (negative η corresponds to the illuminated half and positive η to the dark half of the droplet). The three-dimensional projection of the absorption distribution for irradiation polar angle Θ of 90 deg (black plane) is shown in Fig. 7. Comparison of Fig. 7 to Fig. 3 makes it clear that as the irradiation solid angle increases, the intensity of the back-absorption maximum decreases. This is explained by the extremely localized characteristic of the back-absorption maximum. The points of maximum back absorption for different incident angles do not coincide, and therefore do not add up, whereas the absorption in the illuminated side is distributed and does add up at each point. In the case of irradiation from a black plane, there is no back absorption maximum. This behavior makes Sitarski's approximation[14] of considering the hemispherical absorption distribution equal to the directional absorption distribution multiplied by the total irradiance incident upon the droplet inadequate. However, since the droplet heating regime in spray combustion environments has been verified to be in the slow heating regime,[15] where the nonuniformity is of no importance, his droplet vaporization results should not have been affected appreciably.

Total hemispherical radiation absorption distribution results (at least 1% accuracy for droplets smaller than 50 μm and 5% accuracy for larger droplets) for speherically symmetric irradiation from a blackbody at 1050 and 2000 K are presented in Fig. 8 for water droplets. Using geometrical optics, the absorption distribution results obtained compare well with Harpole's results except for the fact that no internal absorption maxima can be seen for the large droplets.

Figure 9 shows the absorption distribution integrated over the 2.6–15 μm wavelength interval (for decane and several

Table 1 Liquid decane—effect of band absorption

λ interval, μm	$\langle Q \rangle$ (10^7 W/m^3)	Q_{front} (10^7 W/m^3)	Q_{back} (10^7 W/m^3)	Blackbody fraction interval
3.4–4.0	4.38	40.6	51.0	0.163
3.2–4.0 and 6.6–8.2	5.87	42.9	161	0.240
2.6–15.0	7.20	47.4	211	0.786

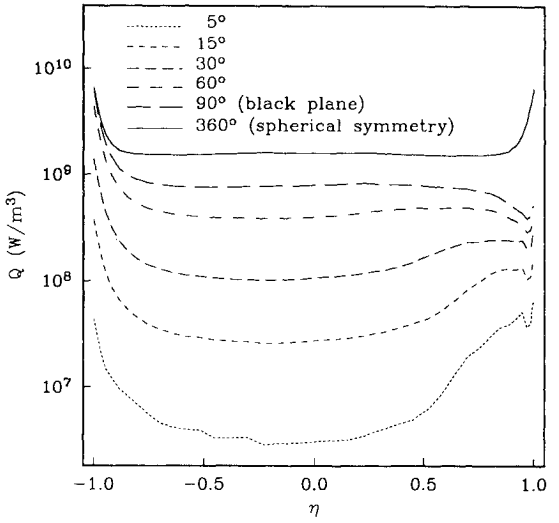

Fig. 6 Total hemispherical absorption distribution for a 50-μm-radius decane droplet irradiated by blackbody radiation at 1500 K within several polar angle values (Θ).

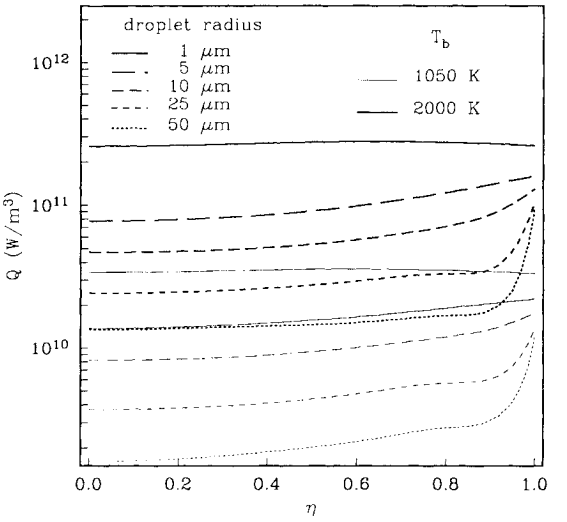

Fig. 8 Total hemispherical absorption distribution for water droplets irradiated by a blackbody at 1050 and 2000 K under spherically symmetric conditions.

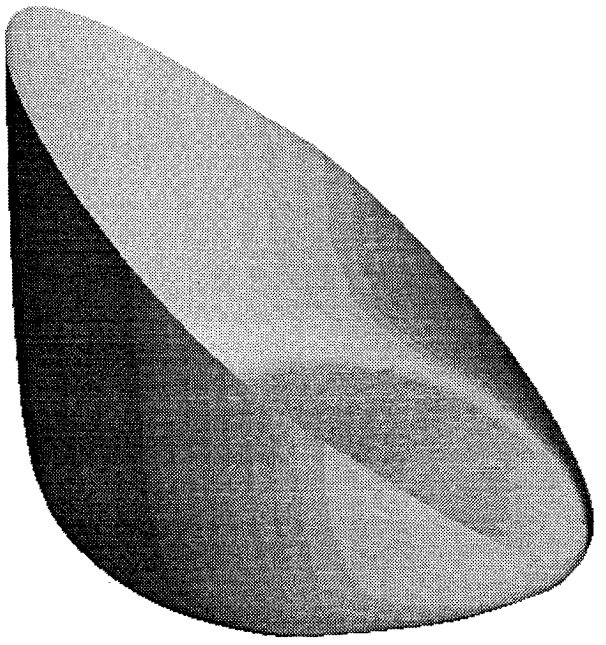

Fig. 7 Total hemispherical absorption distribution for a 50-μm-radius decane droplet irradiated by blackbody radiation at 1500 K within 90-deg polar angle.

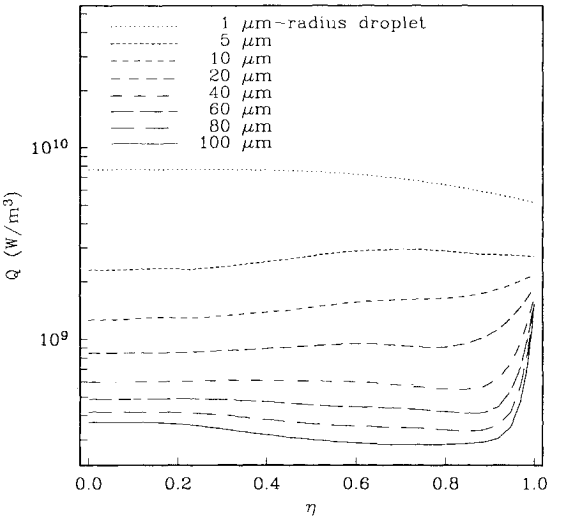

Fig. 9 Total hemispherical absorption distribution for decane droplets irradiated by a blackbody at 1000 K under spherically symmetric conditions.

droplet sizes), for spherically-symmetric blackbody irradiation at 1000 K. In contrast with the water droplet absorption distributions, the decane radiation absorption is more uniformly distributed inside the droplet due to the weaker decane absorptance. However, the absorption distributions do present weak maxima or minima inside the droplet.

The dimensionless absorption distribution $S(\eta)$ for 5- and 50-μm-radius water droplets irradiated by blackbody radiation at several temperatures is shown in Fig. 10. It can be seen that the blackbody temperature does not affect much the absorption profile, which is explained by the strong water absorption over the entire infrared spectral region. Figure 11 shows the dimensionless absorption $S(\eta)$ for various droplet sizes for n-decane irradiated by a blackbody at 1000 K. Although $S(\eta)$ varies appreciably with the droplet size, a linear interpolation in droplet size is reasonable to determine the absorption distribution during droplet vaporization simulations.[15]

Given the complexity of the automatic integrator, one is inclined to investigate the performance of a simpler quadrature scheme to be used in comprehensive spray combustion simulations. Consequently, we now turn to the trapezoidal quadrature investigation. Figure 12 compares the results for directional irradiation for 50-μm-radius decane and water droplets obtained using the automatic integrator with those

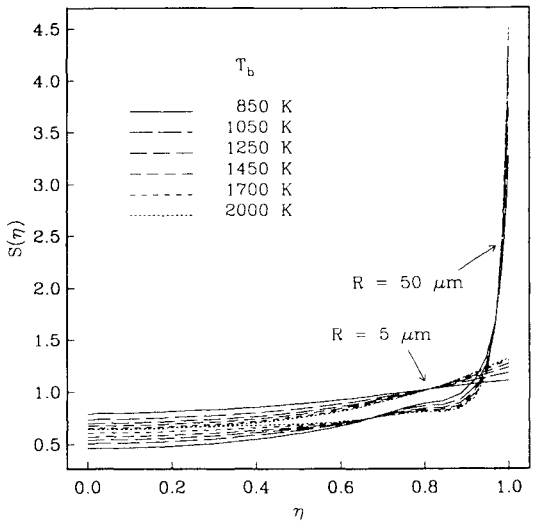

Fig. 10 Dimensionless absorption distribution for 5- and 50-μm-radius water droplets irradiated under spherically symmetric conditions.

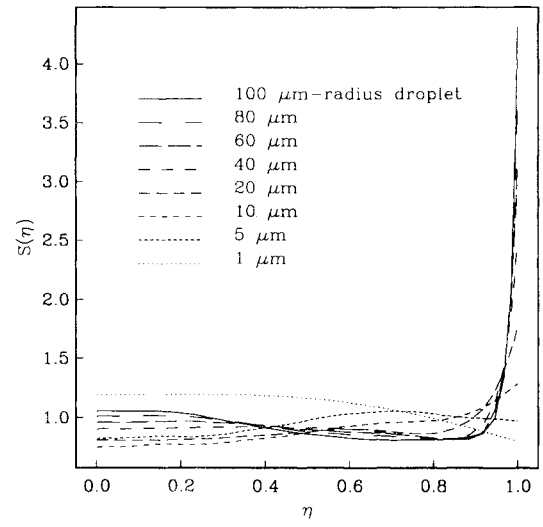

Fig. 11 Dimensionless absorption distribution for decane droplets irradiated by a blackbody at 1000 K under spherically symmetric conditions.

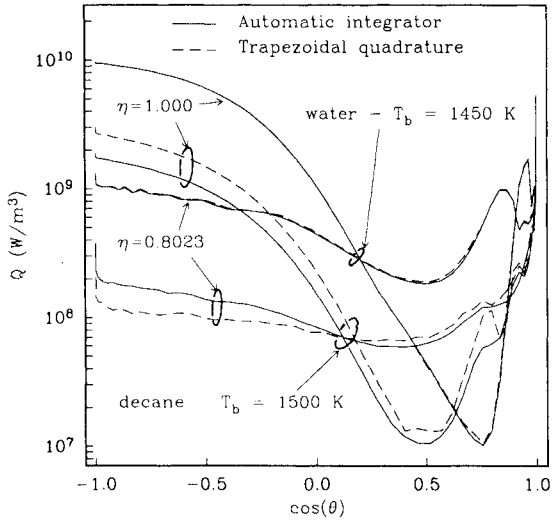

Fig. 12 Absorption distribution for 50-μm-radius water and decane droplets directionally irradiated by blackbody radiation. Comparison between integration schemes.

obtained by trapezoidal quadrature based on tabulated optical constant data (63 data points for decane and 113 for water). It can be seen that the agreement is excellent for water. On the other hand, for decane, the agreement is only reasonable because of the smaller number of data points used in the trapezoidal quadrature computations. It can be seen that for a small number of intervals the trapezoidal rule overestimates the surface absorption, which leads to an underestimation of the absorption inside the droplet. However, the back absorption maximum value is well-predicted. Since the front absorption is mostly due to the bands, the discrepancy in its value was expected because less spectral absorption evaluations are performed inside the bands when only the tabulated data are used.

The total absorptances calculated from the total hemispherical absorption distributions given by trapezoidal quadrature and by the automatic integrator, as well as those obtained by efficiency factor spectral integration, are given in Table 2 for water droplets. The absorptances based on the efficiency-factor spectral integration have been obtained with an accuracy better than 0.1% and are considered to be exact. It should be noticed that the absorptances given in Table 2 are based only on the energy within the blackbody intervals considered, which are also given therein. The agreement between the absorptance values given by the absorption distributions obtained by using the automatic integrator and those obtained by absorption efficiency factor integration are always better than the accuracy obtained in the spectral distribution integrations, that is 1% for radii below 50 μm and 5% for this size. The trapezoidal quadrature results for this total quantity are also good. They agree with the total absorptances given by efficiency factor integration within 5%, with a mean error of around 2%. Thus, trapezoidal quadrature is a good method for calculating total and local absorption values, especially if enough wavelength intervals are used.

Table 3 shows our absorptance values (multiplied by the blackbody fraction), based on the efficiency factor integra-

Table 2 Comparison among methods of total absorptance calculation

	T_b, K					
R, μm	850	1050	1250	1450	1700	2000
	α from radiation absorption distributions					
1	0.1682	0.1708	0.1618	0.1465	0.1243	0.1005
5	0.5115	0.4562	0.4010	0.3468	0.2827	0.2232
10	0.6835	0.5948	0.5137	0.4391	0.3553	0.2790
25	0.8359	0.7314	0.6321	0.5421	0.4416	0.3489
50	0.8796	0.7819	0.6831	0.5906	0.4863	0.3879
	α from absorption distributions (trapezoidal rule)					
1	0.1683	0.1711	0.1621	0.1469	0.1248	0.1009
5	0.5125	0.4579	0.4029	0.3489	0.2848	0.2252
10	0.6857	0.5983	0.5174	0.4431	0.3594	0.2829
25	0.8383	0.7355	0.6374	0.5477	0.4476	0.3546
50	0.8819	0.7859	0.6883	0.5966	0.4929	0.3943
100	0.8959	0.8258	0.7423	0.6567	0.5539	0.4511
	α from efficiency factor spectral integration					
1	0.1666	0.1692	0.1608	0.1458	0.1237	0.1000
5	0.5070	0.4524	0.3988	0.3451	0.2814	0.2221
10	0.6774	0.5899	0.5108	0.4370	0.3536	0.2777
25	0.8286	0.7254	0.6294	0.5402	0.4407	0.3486
50	0.8849	0.7925	0.6996	0.6096	0.5066	0.4076
100	0.9083	0.8358	0.7560	0.6735	0.5742	0.4737
250	0.9177	0.8734	0.8178	0.7534	0.6677	0.5726
500	0.9215	0.8949	0.8578	0.8093	0.7378	0.6515
1000	0.9242	0.9106	0.8891	0.8558	0.7996	0.7245
1500	0.9249	0.9166	0.9022	0.8762	0.8280	0.7596
	Blackbody fraction interval, $\Delta\mathcal{F}$					
—	0.9910	0.9913	0.9944	0.9950	0.9951	0.9951

Table 3 Total absorptances—error of geometric optics approach

R, μm	T_b, K 850	1050	1250	1450	1700	2000
	$\alpha\Delta\mathcal{F}$ from efficiency factor spectral integration					
1	0.1651	0.1677	0.1599	0.1451	0.1231	0.0995
5	0.5024	0.4485	0.3966	0.3434	0.2800	0.2210
10	0.6713	0.5848	0.5079	0.4348	0.3519	0.2763
25	0.8212	0.7191	0.6259	0.5375	0.4386	0.3469
50	0.8770	0.7856	0.6957	0.6065	0.5041	0.4056
100	0.9001	0.8286	0.7517	0.6701	0.5714	0.4714
250	0.9095	0.8658	0.8132	0.7496	0.6645	0.5698
500	0.9132	0.8872	0.8530	0.8052	0.7342	0.6483
1000	0.9159	0.9027	0.8841	0.8515	0.7957	0.7209
1500	0.9166	0.9087	0.8971	0.8718	0.8240	0.7558
	Percent difference between $\alpha\Delta\mathcal{F}$ and Harpole's α_{eff}					
10	−21.0	−19.6	−19.3	−19.0	—	—
25	−13.1	−11.4	−11.0	−9.83	—	—
50	−7.07	−5.80	−5.56	−5.19	—	—
100	−3.23	−2.24	−2.22	−2.10	—	—
250	−0.49	−0.09	−0.52	−0.61	—	—
500	0.53	0.65	0.12	−0.02	—	—
1000	1.20	1.36	0.89	0.76	—	—
1500	1.46	1.68	1.22	1.06	—	—

tion, and the percent difference between them and Harpole's total absorptance results.[11] It can be seen that the absorptances given by Harpole for the same conditions are different from ours by as much as 20%, which is far above the 5% error conjectured by Harpole.[11] However, for droplet radii above 25 μm, the use of geometrical optics and spectral trapezoidal quadrature leads to errors less than 10%, which is reasonable for most engineering calculations. For droplet radii above 100 μm the error is less than 3.5%. Since the absorptances obtained here using trapezoidal quadrature have good accuracy, these errors are due to the geometrical-optics approximation.

Conclusions

Total directional and hemispherical radiation absorption distributions, based on electromagnetic theory results, have been presented for 1–50-μm-radius droplets irradiated by a blackbody at 850, 1050, 1250, 1450, 1700, and 2000 K, and for 1–100-μm-radius decane droplets irradiated by a blackbody at 1000 and 1500 K (with wavelength interval limitation). Total absorption distributions have also been determined by trapezoidal quadrature spectral integration in order to check its applicability. For water (under the same conditions) the total absorptance has been calculated from the total hemispherical absorption distributions, from direct integration of the absorption efficiency factor and from the approximation for the total hemispherical absorption distribution given by spectral integration by trapezoidal rule. The total absorptance for water droplets of up to 1500 μm radius has also been calculated using the efficiency factor integration. These results have been compared to Harpole's geometrical-optics absorptances. For the above cases, the following has been verified:

1) The consideration of the two decane principal bands, including their wings, at the wavelengths of 3.4 and 6.8 μm can represent the decane absorption distribution moderately well. This finding indicates a simple band model for liquid decane absorption.

2) Although the total directional absorption distribution can be appreciably back-concentrated, the total hemispherical absorption distribution is primarily front-concentrated, because the back absorption maximum decreases markedly as the irradiation solid angle increases for the conditions analyzed.

3) The total hemispherical absorption radial profile varies little with the blackbody temperature for a given droplet size for spherically-symmetric irradiation.

4) The use of trapezoidal quadrature for the spectral integration introduces very small error in the total absorption distribution and absorptance calculations (usually 1–3%, for water using 112 intervals).

5) The geometrical-optics approximation can introduce more than 20% of error in the absorptance calculation for droplets smaller than 10 μm in radius, for the conditions analyzed; however, this error drops rapidly as the droplet size increases, so that there is less than a 10% error for droplets larger than 25 μm, and less than a 6% error for droplets above 50 μm in radius.

Acknowledgments

P. L. C. Lage would like to acknowledge the financial support from CNPq, Grant 202129/90.0. This research was supported in part by the University of California Irvine through an allocation of computer resources. The authors also acknowledge the assistance of A. V. Schiano and S. D. Franklin in developing the three-dimensional graphic projections. D. K. Edwards read the original manuscript and provided useful comments.

References

[1]Faeth, G. M., "Evaporation and Combustion of Sprays," *Progress in Energy and Combustion Science*, Vol. 9, 1983, pp. 1–76.

[2]Law, C. K., "Recent Advances in Droplet Vaporization and Combustion," *Progress in Energy and Combustion Science*, Vol. 8, No. 3, 1982, pp. 169–199.

[3]Sirignano, W. A., "Fuel Droplet Vaporization and Spray Combustion Theory," *Progress in Energy and Combustion Science*, Vol. 9, No. 4, 1983, pp. 291–322.

[4]Rangel, R. H., "Heat Transfer in Vortically-Enhanced Mixing of Vaporizing Droplet Sprays," *Annual Review of Heat Transfer*, Vol. VI, edited by C. L. Tien, Hemisphere, New York, 1991, Chap. 7, pp. 331–362.

[5]Abramzon, B., and Sirignano, W. A., "Droplet Vaporization Model for Spray Combustion Calculations," *International Journal of Heat and Mass Transfer*, Vol. 32, Sept. 1989, pp. 1605–1618.

[6]Tong, A. Y., and Sirignano, W. A., "Multicomponent Droplet Vaporization in a High Temperature Gas," *Combustion and Flame*, Vol. 66, 1986, pp. 221–235.

[7]Dusel, P. W., Kerker, M., and Cooke, D. D., "Distribution of Absorption Centers Within Irradiated Spheres," *Journal of the Optical Society of America*, Vol. 69, Jan. 1979, pp. 55–59.

[8]Pendleton, J. D., "Water Droplets Irradiated by a Pulsed CO_2 Laser: Comparison of Computed Temperature Contours with Explosive Vaporization Patterns," *Applied Optics*, Vol. 24, June 1985, pp. 1631–1637.

[9]Kafalas, P., and Ferdinand, A. P., Jr., "Fog Droplet Vaporization and Fragmentation by a 10.6-μm Laser Pulse," *Applied Optics*, Vol. 12, 1973, pp. 29–33.

[10]Tuntomo, A., Park, S. H., and Tien, C. L., "Internal Distribution of Radiant Absorption in a Spherical Particle," *Journal of Heat Transfer*, Vol. 113, May 1990, pp. 407–412.

[11]Harpole, G. M., "Radiative Absorption by Evaporating Droplets," *International Journal of Heat and Mass Transfer*, Vol. 23, 1980, pp. 17–26.

[12]Mackowski, D. W., Altenkirch, R. A., and Menguc, M. P., "Internal Absorption Cross Sections in a Stratified Sphere," *Applied Optics*, Vol. 29, April 1990, pp. 1551–1559.

[13]Sitarski, M. A., "On the Feasibility of Secondary Atomization of Small Slurry Droplets Exposed to Intense Thermal Radiation," *Combustion Science and Technology*, Vol. 54, 1987, pp. 177–201.

[14]Sitarski, M. A., "Thermal Dynamics of a Small Vaporizing Slurry Droplet in a Hot and Radiant Environment; Feasibility of the Secondary Atomization," *Combustion Science and Technology*, Vol. 71, Nos. 1–3, 1990, pp. 53–75.

[15]Lage, P. L. C., and Rangel, R. H., "Single Droplet Vaporization Including Thermal Radiation Absorption," *Journal of Thermophysics and Heat Transfer* (to be published).

[16]Bohren, C. F., and Huffman, D. R., *Absorption and Scattering of Light by Small Particles*, Wiley, New York, 1983, pp. 82–104.

[17]Mackowski, D. W., "Photophoresis of Aerosol Particles in the Free Molecular and Slip-Flow Regimes," *International Journal of Heat and Mass Transfer*, Vol. 32, May 1989, pp. 843–854.

[18]Wiscombe, W. J., "Improved Mie Scattering Algorithms," *Applied Optics*, Vol. 19, May 1980, pp. 1505–1509.

[19]Lentz, W. J., "Generating Bessel Functions in Mie Scattering Calculations Using Continued Fractions," *Applied Optics*, Vol. 15, March 1976, pp. 668–671.

[20]Patterson, T. N. L., "The Optimum Addition of Points to Quadrature Formulae," *Mathematics of Computation*, Vol. 22, 1968, pp. 847–856; see also Vol. 23, 1969, pp. 892.

[21]Patterson, T. N. L., "Algorithm for Automatic Numerical Integration over a Finite Interval, Algorithm 468," *Communications of the Association for Computing Machinery*, Vol. 11, No. 11, 1973, pp. 694–699.

[22]Davis, P. J., and Rabinowitz, P., "Methods of Numerical Integration," 2nd ed., Academic Press, New York, 1984, pp. 98, 99.

[23]Hale, G. M., and Querry, M. R., "Optical Constants of Water in the 200-nm to 200-μm Wavelength Region," *Applied Optics*, Vol. 12, March 1973, pp. 555–563.

[24]Tuntomo, A., "Transport Phenomena in a Small Particle with Internal Radiant Absorption," Ph.D. Dissertation, Univ. of California at Berkeley, Berkeley, CA, 1990.